

Structural Insight into the Pharmacophore Pocket of Human Glutamate Carboxypeptidase II[†]

Cyril Bařinka,[†] Miroslava Rovensk,^{‡,§} Petra Mlochov,^{‡,§} Klara Hlouchov,^{‡,§} Anna Plechanovov,^{‡,§} Pavel Majer,[#] Takashi Tsukamoto,[#] Barbara S. Slusher,[#] Jan Konvalinka,^{‡,§} and Jacek Lubkowski^{*,†}

Center for Cancer Research, National Cancer Institute at Frederick, Frederick, Maryland 21702, Gilead Sciences and IOCB Research Centre, Institute of Organic Chemistry and Biochemistry, Academy of Sciences of the Czech Republic, Flemingovo n. 2, Prague, Czech Republic, Department of Biochemistry, Faculty of Natural Science, Charles University, Hlavova 2030, Prague, Czech Republic, and MGI Pharma, Inc., 6611 Tributary Street, Baltimore, Maryland 21224

Received February 2, 2007

Inhibition of glutamate carboxypeptidase II (GCPII) has been shown to be neuroprotective in multiple preclinical models in which dysregulated glutamatergic transmission is implicated. Herein, we report crystal structures of the human GCPII complexed with three glutamate mimetics/derivatives, 2-(phosphonomethyl)pentanedioic acid (2-PMPA), quisqualic acid (QA), and L-serine O-sulfate (L-SOS), at 1.72, 1.62, and 2.10 Å resolution, respectively. Despite the structural differences between the distal parts of the inhibitors, all three compounds share similar binding modes in the pharmacophore (i.e., S1') pocket of GCPII, where they are stabilized by a combination of polar and van der Waals interactions. The structural diversity of the distal parts of the inhibitors leads to rearrangements of the S1' site that are necessary for efficient interactions between the enzyme and an inhibitor. The set of structures presented here, in conjunction with the available biochemical data, illustrates a flexibility of the GCPII pharmacophore pocket and highlights the structural features required for potent GCPII inhibition. These findings could facilitate the rational structure-based drug design of new GCPII inhibitors in the future.

1. Introduction

The development of novel neuroprotective agents attracts considerable interest because the existing therapies often lack desired efficacy and selectivity.¹ One recently identified pharmacologically exploitable target/marker protein is glutamate carboxypeptidase II (GCPII,⁴ EC 3.4.17.21), a membrane-bound metalloproteinase expressed predominantly in the human nervous system, the brush border of the small intestine, proximal renal tubules, and prostate parenchyma.^{2,3} Within the nervous system, GCPII is expressed primarily on astrocyte and Schwann cell membranes with the catalytic ectodomain facing the extracellular milieu. There, it hydrolyzes *N*-acetylaspartylglutamate (NAAG), the most abundant neuropeptide in the mammalian brain, and liberates free glutamate.⁴ Excessive (or dysregulated) glutamatergic transmission is associated with various pathophysiologies including traumatic brain injury, stroke, neuropathic and inflammatory pain, amyotrophic lateral sclerosis (ALS), and schizophrenia.^{5–8} NAAG itself is an agonist at the group II metabotropic glutamate receptors (mGluR3) on glia and neurons.⁹ Activation of mGluR3

affects a wide spectrum of cellular functions, including the release of neuroprotective trophic factors or the inhibition of glutamate release.^{10,11} Consequently, the inhibition of GCPII provides protection in the animal models presumably because of decreasing levels of free glutamate and increasing NAAG concentrations.

GCPII has a strong preference for substrates with glutamate at the C-terminal position.¹² Not surprisingly then, the first GCPII inhibitors identified were glutamate/NAAG mimetics/derivatives, such as quisqualic acid (QA) and *N*-fumaryl glutamate.^{13,14} Demands for a more specific and potent inhibitor were met by the synthesis of 2-(phosphonomethyl)pentanedioic acid (2-PMPA, $K_i = 0.3$ nM),¹⁵ which is currently one of the most extensively studied GCPII inhibitors. Subsequently, many novel GCPII-specific compounds of different chemistries have been designed and synthesized. At present, most of the substrate-based GCPII inhibitors include a glutamate moiety linked to a zinc-binding group such as phosphonate, phosphinate, hydroxamate, urea, phosphoamidate, and thiol.^{16–20} Additionally, despite the presumed low tolerance of the GCPII pharmacophore pocket for the structural changes of an inhibitor, conformationally constrained NAAG mimetics or P1'-carboxylbenzyl-containing analogues were shown to possess inhibitory activity toward GCPII.^{21,22}

Recently reported crystal structures of GCPII revealed that the extracellular part of the enzyme is organized into the three domains spanning amino acids 57–116 and 352–590 (the protease-like domain), 117–351 (the apical domain), and 591–750 (the C-terminal domain) and that amino acid residues from all the three domains are required for high-affinity substrate/inhibitor binding.^{23,24} These structural findings, in conjunction with SAR analysis reported previously, provided useful information for the rational structure-based design of new GCPII inhibitors.

Available crystallographic data on GCPII represent a major step toward our understanding of structural features of the

[†] Accession numbers: Atomic coordinates of the present structures together with the experimental diffraction amplitudes have been deposited at the RCSB Protein Data Bank with accession numbers 2PVW (the complex with 2-PMPA), 2OR4 (the complex with quisqualate), and 2PVV (the complex with L-serine O-sulfate).

* To whom correspondence should be addressed. Address: Macromolecular Crystallography Laboratory, 539 Boyles Street, National Cancer Institute at Frederick, Frederick, Maryland 21702. Phone: 301-846-5494. Fax: 301-846-7517. E-mail: jacek@ncifcrf.gov.

[†] National Cancer Institute at Frederick.

[‡] Academy of Sciences of the Czech Republic.

[§] Charles University.

[#] MGI Pharma.

⁴ Abbreviations: GCPII, glutamate carboxypeptidase II; NAAG, *N*-acetyl-L-aspartyl-L-glutamate; 2-PMPA, (*R,S*)-2-(phosphonomethyl)pentanedioic acid; QA, quisqualic acid, 2-amino-3-(3,5-dioxo[1,2,4]oxadiazolidin-2-yl)propionic acid; rhGCPII, recombinant human glutamate carboxypeptidase II; PEG, polyethylene glycol; AMPA, 2-amino-3-(3-hydroxy-5-methyl-4-isoxazolyl)propionic acid; Glu, glutamic acid; SAR, structure-activity relationship; PSMA, prostate-specific membrane antigen; L-SOS, L-serine O-sulfate; L-SOP, L-serine O-phosphate; K_i , inhibition constant.

Table 1. Data Collection and Refinement Statistics

	rhGCPII/2-PMPA	rhGCPII/QA	rhGCPII/L-SOS
Data Collection Statistics			
wavelength (Å)	1.000	1.000	1.5478
space group	<i>I</i> 222	<i>I</i> 222	<i>I</i> 222
unit-cell parameters <i>a</i> , <i>b</i> , <i>c</i> (Å)	101.8, 130.8, 159.4	102.0, 130.4, 159.5	101.6, 130.2, 159.0
resolution limits (Å)	30.0–1.72 (1.78–1.72) ^a	50.0–1.62 (1.68–1.62) ^a	30.0–2.10 (2.18–2.10) ^a
no. of unique reflections	111281 (10238)	129603 (9922)	60304 (5928)
redundancy	9.8 (6.0)	11.0 (5.7)	4.8 (4.8)
completeness (%)	98.6 (91.7)	96.7 (74.8)	98.9 (98.4)
<i>I</i> / σ (<i>I</i>)	15.1 (3.5)	28.2 (2.7)	15.4 (3.7)
<i>R</i> _{merge}	0.126 (0.495)	0.070 (0.465)	0.097 (0.505)
Refinement Statistics			
resolution limits (Å)	15.0–1.72 (1.76–1.72)	30.0–1.62 (1.66–1.62)	30.0–2.10 (2.16–2.10)
total no. of reflections	105604	123053	57236
no. of reflections in working set	100055 (5998)	116532 (6550)	54175 (3972)
no. of reflections in test set	5549 (344)	6521 (360)	3061 (217)
<i>R</i> / <i>R</i> _{free}	0.183 (0.232)/0.207 (0.288)	0.185 (0.272)/0.218 (0.337)	0.176 (0.203)/0.212 (0.274)
total no. of non-H atoms	6217	6825	6329
no. of non-H protein atoms	5678	5871	5804
no. of ions	4	4	4
no. of water molecules	521	937	510
average <i>B</i> factor (Å ²)			
protein atoms	34.0	25.6	29.2
waters	43.1	39.9	36.3
inhibitor	30.7	23.8	25.1
rmsd			
bond length (Å)	0.019	0.019	0.021
bond angle (deg)	1.80	1.79	1.80
planarity (Å)	0.009	0.009	0.009
chiral center (Å ³)	0.132	0.124	0.125
gaps in the structure	42–55, 541–543, 654–655	42–55, 152–155, 541–543	42–55, 654–655

^a Values in parentheses correspond to the highest resolution shells.

enzyme, but the insight into the S1' (i.e., pharmacophore) pocket of GCPII is still quite limited. This is due to the fact that all available X-ray structures of GCPII have the S1' site either empty or occupied by a glutarate moiety. To obtain deeper understanding of the flexibility of the S1' pocket and to define the structural features required for potent GCPII inhibition more precisely, we determined crystal structures of human GCPII in complex with three glutamate analogues/mimetics harboring distinct S1' binding moieties. The set of structures presented here characterizes structural adjustments of the S1' pocket that are necessary to accommodate inhibitors with varied moieties in the P1' position. The availability of the crystallographic data on GCPII complexed structurally diversified inhibitors could thus facilitate development of novel GCPII specific inhibitors with enhanced activity in the future.

2. Experimental Section

2.1. Inhibitors. QA (2-amino-3-(3,5-dioxo[1,2,4]oxadiazolidin-2-yl)propionic acid) was obtained from Fluka (Fluka, 99% TLC). The stock solution was prepared by dissolving 1 mg of the inhibitor in 66 μ L of 100 mM NaOH (80 mM final concentration). (*R,S*)-2-(phosphonomethyl)pentanedioic acid (2-PMPA, a racemic form) was synthesized as described previously,¹⁵ and the inhibitor was dissolved in distilled water to a final concentration of 50 mM. L-Serine *O*-sulfate (L-SOS), L-serine *O*-phosphate (L-SOP), and (*S*)-willardiine were purchased from Sigma (St. Louis, MO).

2.2. rhGCPII Expression and Purification. The extracellular domain of human glutamate carboxypeptidase II (rhGCPII, amino acids 44–750) was overexpressed in *Drosophila* Schneider S2 cells and purified to homogeneity as described previously.¹² The protein was dialyzed against 20 mM Tris-HCl, 100 mM NaCl, pH 8.0, and concentrated to 10 mg/mL using an YM50 Centricon ultrafiltration device (Millipore). The protein concentration was determined with the Bio-Rad protein assay kit, using the bovine serum albumin as a standard.

2.3. Crystallization and Data Collection. The protein solution was mixed with the inhibitor stock solutions at 10:1 ratio

(resulting in an approximate 50-fold molar excess of the inhibitor), and the droplets were set up by combining 2 μ L of the rhGCPII-inhibitor mixture and 2 μ L of the reservoir solution containing 33% (v/v) pentaerythritol propoxylate PO/OH 5/4, 1–3% (w/v) PEG 3350, and 100 mM Tris-HCl, pH 8.0. The orthorhombic crystals of approximately 0.4 mm \times 0.4 mm \times 0.2 mm (*I*222 space group with one rhGCPII molecule per asymmetric unit) were grown using the hanging drop vapor diffusion method at 293 K, typically within 1 week. For the X-ray experiments, crystals were frozen in a stream of liquid nitrogen directly from hanging drops. The diffraction data for rhGCPII/2-PMPA and rhGCPII/QA were collected at 100 K using synchrotron radiation at the SER-CAT beamlines (sectors 22BM and 22ID) at the Advanced Photon Source (Argonne, IL) with the X-ray wavelength of 1.0 Å, and the images were recorded on MAR charge-coupled device detectors. The diffraction data for the rhGCPII/L-SOS complex were collected in-house at 100 K using X-radiation ($\lambda_{\text{Cu}} = 1.5478$ Å) generated by the rotating anode operating at 100 kV and 50 mA (Rigaku-Ru200), and reflection intensities were recorded on the MAR345 image plate detector (MAR Research, Hamburg, Germany). In all cases, the diffraction intensities were collected from single crystals and processed using the HKL2000 software package.²⁵

2.4. Structure Determination and Refinement. Since the crystals of rhGCPII/inhibitor complexes were isomorphous with a previously reported crystal of the ligand-free rhGCPII,²⁶ this structure (RSCB PDB code 2OOT) served as the initial solution. The structures were refined and manually rebuilt using the programs Refmac5²⁷ and Xtalview,²⁸ respectively. During the refinement, 5% of the randomly selected reflections were kept aside for cross-validation (*R*_{free}). The quality of the final models was evaluated using the program PROCHECK²⁹ distributed with the CCP4i suite, version 2.2.³⁰ Ramachandran analysis of the final models classified all residues but one, Lys207, as having either the most favorable or allowed conformations. Despite supposedly unfavorable conformations, all atoms of Lys207 are well defined in the electron density peaks. The final statistics for the data collection and the structure refinement are summarized in Table 1.

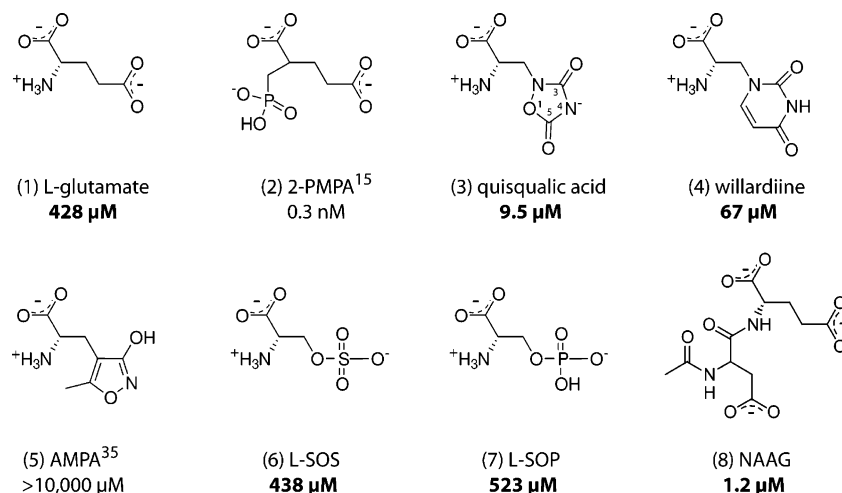


Figure 1. Chemical definitions of glutamate analogues: (1) L-Glu; (2) 2-PMPA, (*R,S*)-2-phosphonomethylpentanedioic acid; (3) quisqualic acid, 2-amino-3-(3,5-dioxo[1,2,4]oxadiazolidin-2-yl)propionic acid; (4) willardiine, 2-amino-3-(2,4-dioxo-3,4-dihydro-2*H*-pyrimidin-1-yl)propionic acid; (5) AMPA, 2-amino-3-(3-hydroxy-5-methyl-4-isoxazolyl)propionic acid; (6) L-SOS, L-serine *O*-sulfate; (7) L-SOP, L-serine *O*-phosphate; (8) NAAG, *N*-acetylaspartylglutamate. Inhibition concentration values (and the K_M value in the case of NAAG) are taken from the published data^{15,37} or determined in our laboratory (shown in bold).

2.5. Determination of Inhibition Concentration Values (IC_{50}).

The inhibition concentration values of rhGCPII were determined using the radioenzymatic assay with [³H]NAAG (radiolabeled on the terminal glutamate). Briefly, rhGCPII (30 ng/mL) was preincubated in the presence of increasing concentrations of inhibitors in 50 mM MOPS, 20 mM NaCl, pH 7.4, for 15 min at 37 °C. The reaction was initiated by adding 20 μL of the mixture of 0.95 μM NAAG (Sigma) and 50 nM [³H]NAAG (50 Ci/mmol in Tris buffer, Perkin-Elmer) to a total reaction volume of 200 μL. After 20 min, the reaction was terminated by adding 200 μL of 200 mM potassium phosphate solution, pH 7.4. The glutamate was separated from the reaction mixture by ion-exchange chromatography and quantified by liquid scintillation. Duplicate reactions were carried out for each experimental point. The IC_{50} values were calculated from plots of v_i/v_0 (ratio of individual reaction rates to the rate of an uninhibited reaction) versus inhibitor concentration using the GraFit program (version 5.0.4, Erithacus Software Limited).

2.6. Mode of rhGCPII Inhibition by Quisqualate (QA). By use of 0.16–40 μM NAAG and QA concentrations of 0, 26, and 75 μM, the mode of inhibition was determined in the reaction setup described above. Initial inhibition velocities for each concentration point were measured in duplicate, and the mode of inhibition was determined from the double-reciprocal plot of velocity versus substrate concentration.

3. Results

3.1. Overall Structure Comparison. The structures of rhGCPII/2-PMPA, rhGCPII/QA, and rhGCPII/L-SOS were refined at resolutions of 1.72, 1.62, and 2.10 Å with crystallographic *R* factors equal to 0.183 ($R_{free} = 0.207$), 0.185 ($R_{free} = 0.218$), and 0.176 ($R_{free} = 0.212$), respectively (Table 1). The overall fold of rhGCPII in all three structures is nearly identical, as illustrated by the root-mean-squared deviation of 0.19 Å (for the 685 equivalent C α pairs), 0.23 Å (for the 690 equivalent C α pairs), and 0.21 Å (for the 692 equivalent C α pairs) between the ligand-free rhGCPII structure and rhGCPII/2-PMPA, rhGCPII/QA, and rhGCPII/L-SOS complexes, respectively.

3.2. Inhibitor Interactions in the S1' Pocket. As glutamate mimetics/derivatives, L-SOS, QA, and 2-PMPA each bind to the S1' pocket of GCPII in a mode similar to that of glutamate. In all complexes, the positive peaks in the $F_o - F_c$ maps clearly showed the location of the inhibitor molecules as well as the surrounding residues from the enzyme (Figure 2).

3.2.1. rhGCPII/2-PMPA Complex. The glutarate fragment of 2-PMPA forms six hydrogen bonds with the side chains of

Arg210, Asn257, Tyr552, Lys699, and Tyr700. Additional hydrogen bonds (2.6 and 2.5 Å) are formed by the α - and γ -carboxylate groups of 2-PMPA and the water molecules. Two oxygen atoms of the inhibitor phosphonate moiety coordinate the active-site Zn²⁺ ions with the Zn \cdots O–P distances of 2.0 and 2.1 Å. Furthermore, one of the phosphonate oxygen atoms forms H-bonds with the hydroxyl group of Tyr552 (2.7 Å) and N ϵ 2 of His553 (3.1 Å). The second phosphonate oxygen interacts with the carboxylate groups of Glu424 (2.8 and 3.2 Å), Asp453 (3.1 Å), and N ϵ 2 of His377 (3.3 Å). The third phosphonate oxygen is stabilized by a weak H-bond with the side chain amide of Asn519 (3.4 Å). The intermolecular contacts between 2-PMPA and rhGCPII are schematically depicted in Figure 3A (and Figure S1 of Supporting Information), and the inhibitor–protein distances are listed in Table T1 in Supporting Information.

3.2.2. rhGCPII/QA Complex. QA is a mimetic of glutamate in which the γ -carboxylate of glutamate is replaced by the 1,2,4-oxadiazolidine ring (Figure 1). In the rhGCPII/QA complex, the α -carboxylate group of QA interacts with the side chains of Arg210, Tyr552, and Tyr700 in a fashion similar to that described for the rhGCPII/2-PMPA complex. The free amino group of quisqualate interacts with the Glu424 γ -carboxylate, the main chain carbonyl group of Gly518, and two water molecules. The oxadiazolidine ring is wedged between Gly427, Leu428, and Gly518 on one side and the side chain of Phe209 on the opposite side of the pharmacophore pocket. Two H-bonds formed by the γ -carboxyl group of 2-PMPA with Lys699 and Asn257 are also present in the QA complex through the ring nitrogen atom N4 (N4 \cdots N ϵ 1, 3.2 Å) and the carbonyl oxygen at position 3 (O3 \cdots N δ 2, 2.8 Å), respectively. Each of these atoms is also hydrogen-bonded to a water molecule that is furthermore stabilized by its interactions with the Leu259 carbonyl oxygen (3.2 Å) and the side chains of Asn257 and Lys699. Additionally, the exocyclic oxygen bound to C5 accepts hydrogen bonds from the main-chain amide of Gly518 (2.9 Å) and from the hydroxyl group of Ser517 (3.3 Å, Figure 3B and Supporting Information Figure S2 and Table T2). To accommodate the bulky oxadiazolidine ring, the S1' pocket of GCPII undergoes a subtle rearrangement. Compared to the rhGCPII/2-PMPA complex, the side chain of Asn257 is rotated by 70° (with a positional difference of 2.2 Å for N δ 2 atoms) and the

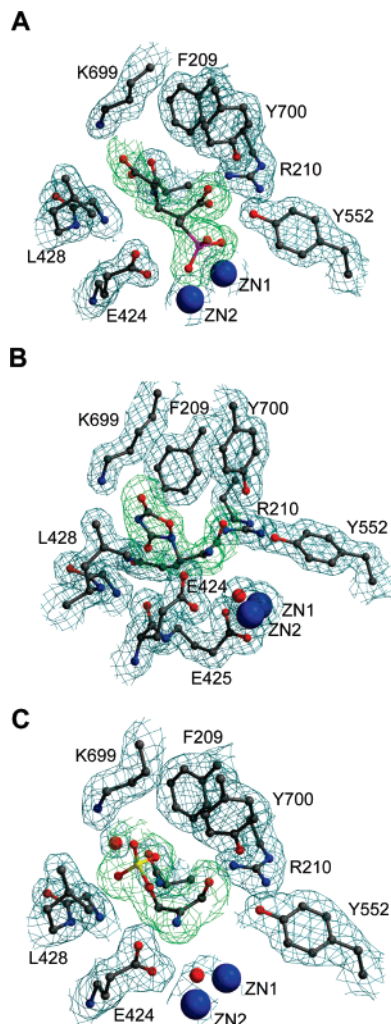


Figure 2. Representative electron density maps of the S1' site in rhGCPII: S1'-bound 2-(S)-PMPA (A), QA (B), and L-SOS (C). Selected amino acids of GCPII are shown in ball-and-stick representation, while Zn²⁺ ions are depicted as blue spheres. The $F_o - F_c$ omit electron density map around an inhibitor is contoured at the 2σ level (green) and the $2F_o - F_c$ difference electron density map at the 1σ level (blue). The picture was generated using MOLSCRIPT⁴¹ and Bobscrip⁴² and rendered with PovRay.⁴³

loop containing Gly518 is displaced from its native conformation in the S1' site (Figure 3D).

3.2.3. rhGCPII/L-SOS Complex. The binding mode of L-SOS in the S1' pocket of rhGCPII is analogous to the QA binding described above. The α -amino acid fragments of both ligands structurally overlap and are stabilized by a similar set of interactions with the enzyme (Figure 3C and Supporting Information Figure S3 and Table T3). The distal sulfate group could be superimposed onto the QA oxadiazolidine ring; its oxygen atoms interact with the amino groups of Lys699 (O2 \cdots N ϵ 1, 3.0 Å) and Asn257 (O1 \cdots N δ 2, 2.9 Å) and are further hydrogen-bonded to a water molecule (O1 \cdots O, 3.1 Å; O3 \cdots O, 3.0 Å). L-SOS features a tetragonal configuration at the sulfur atom in place of the planar QA oxadiazolidine ring or planar configuration at the glutamate C δ . This spatial arrangement elicits slight movement of the Phe209 side chain to avoid possible steric clashes (Figure 3D).

3.3. Inhibition Concentration Values of Glutamate Mimetics. Inconsistent results have been reported regarding the inhibition mode and potency of QA as an inhibitor of GCPII.^{31,32} We determined that QA is a competitive inhibitor of GCPII with an inhibition concentration of 9.5 μ M (Figures 1 and 4).

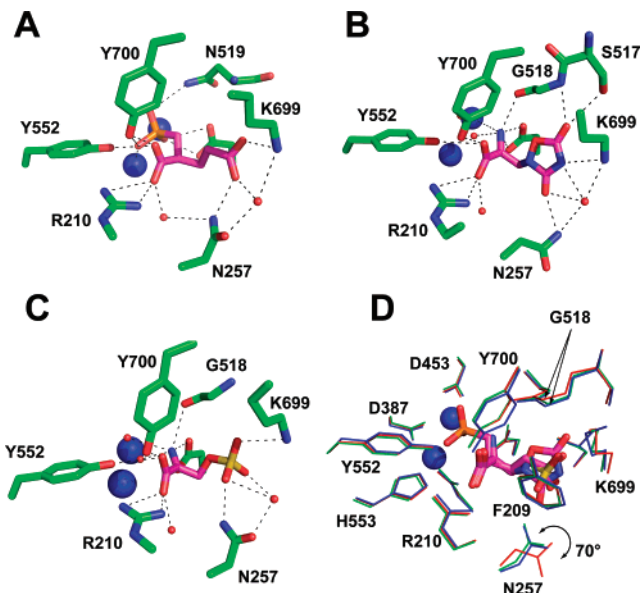


Figure 3. Inhibitor binding to the S1' pocket of rhGCPII: schematic representation of the S1' pocket of rhGCPII complexed with 2-(S)-PMPA (A), QA (B), and L-SOS (C). The N, O, and P atoms are colored in blue, red, and orange, respectively. The carbon atoms are shown in green (rhGCPII) or magenta (the S1'-bound QA/2-PMPA/L-SOS). The Zn²⁺ ions and water molecules are represented by the blue and red spheres, respectively. Hydrogen-bonding interactions between the S1'-bound inhibitor(s) and the rhGCPII residues are shown as dashed lines. The H-bonding distances are summarized in Supporting Information Tables T1–T3. The superposition of the rhGCPII S1' sites observed in complex with 2-PMPA, QA, and L-SOS is shown in panel D. The residues in the rhGCPII/2-PMPA, rhGCPII/QA, and rhGCPII/L-SOS complexes are shown in green, red, and blue, respectively. Note the rotation of the Asn257 side chain and slight shift of Phe209, Gly518, Lys699, and Tyr700. The picture was generated using PyMOL.⁴⁴

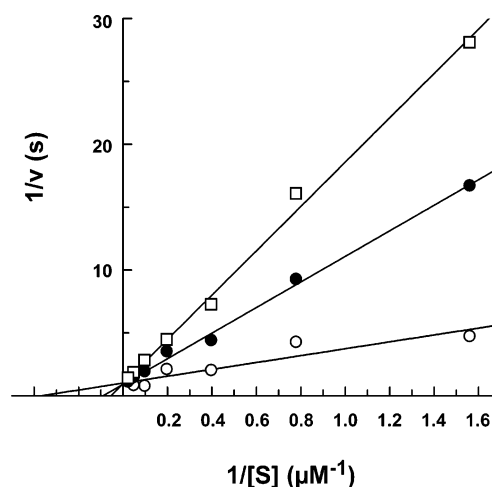


Figure 4. Double-reciprocal plot depicting inhibition mechanism of rhGCPII by quisqualate (QA). The mode of inhibition was determined by measuring rhGCPII hydrolyzing activity at a NAAG concentration range of 0.16–40 μ M, in the absence (○) or in the presence of 26 μ M QA (●) or 75 μ M QA (□), employing the radioenzymatic assay described in the Experimental Section.

These biochemical findings are in agreement with the structural data presented here that clearly show the QA binding to the S1' pocket of rhGCPII. Furthermore, the results of our kinetic experiments demonstrate that compared to QA, glutamate, L-SOS, and L-serine *O*-phosphate are at least 50 times less potent inhibitors of rhGCPII with IC₅₀ values of 428, 438, and 523 μ M, respectively (Figure 1).

4. Discussion

At present, 2-PMPA is the most extensively studied inhibitor of GCPII, with proven efficacy in models of ischemic brain injury, neuropathic pain, and amyotrophic lateral sclerosis (for a review, see ref 4). The superposition of the rhGCPII/2-PMPA structure with the rhGCPII/glutamate and rhGCPII/GPII8431 complexes published recently²⁴ reveals that the binding modes of the glutamate fragments of these compounds within the S1' pocket are virtually identical. Yet the inhibitory potencies of the three compounds span more than 6 orders of magnitude with K_I values of 0.3 nM, ~100 nM, and 428 μ M for 2-PMPA, GPII8431, and glutamate, respectively. Consequently, the higher affinity of 2-PMPA against GCPII can only be attributed to the strong interactions between the active site zinc ions and the phosphonate moiety as well as a set of supplementary interactions between the phosphonate and the enzyme.

In general, the replacement of a phosphonate oxygen of 2-PMPA by an alkyl/aryl functionality increases inhibition constants of such derivatives more than 100-fold.¹⁸ In the rhGCPII/2-PMPA complex, the "extra" phosphonate oxygen/hydroxyl group (replaced by a methylene group in phosphinate compounds) forms a weak hydrogen bond with the side chain amide of Asn519. Although this interaction might partially contribute to a higher affinity of 2-PMPA, it is more likely that other factors play an even more prominent role. It should be noted that the phosphonate group of 2-PMPA could release two protons in aqueous solutions (reaching a formal charge of -2), with the calculated values $pK_{a1} \approx 1.8$ and $pK_{a2} \approx 8.5$. It is plausible that under physiological conditions both oxygen atoms of phosphonate will be deprotonated in the vicinity of the active-site zinc ions. As a result, the doubly negatively charged phosphonate group ($R-PO_3^{2-}$) could interact with the positively charged zinc ions with greater avidity than the phosphinate group ($R_{1,2} = PO_2^{1-}$), thus contributing to the observed increased potency of phosphonate versus phosphinate compounds.

Results reported by Vitharana et al.³³ indicate that the potent inhibition of GCPII is attributable only to the (*S*)-form of the two 2-PMPA enantiomers, whose absolute configuration is analogous to L-glutamate and is >300 times more active than the (*R*)-enantiomer. Consistent with this report, only 2-(*S*)-PMPA was detected in the structure of rhGCPII/2-PMPA described here, even though the protein was cocrystallized with the racemic form of 2-PMPA. To explain the different activities of the two 2-PMPA enantiomers, we constructed a model of the rhGCPII/2-(*R*)-PMPA complex based on the structure of rhGCPII/2-(*S*)-PMPA complex (data not shown). Assuming that the binding mode of the phosphonate group in the GCPII active site is the same for both enantiomers, the inversion of groups around the C α (glutamate) atom in 2-(*R*)-PMPA prevents interaction between the C α -carboxylate of the ligand and the Arg210 of the enzyme. Furthermore, the same carboxylate group becomes closely positioned to the negatively charged Glu425 γ -carboxylate, resulting in steric clashes and charge repulsions. According to our model, a more complex rearrangement of the GCPII active site would be needed to accommodate the (*R*)-enantiomer, which would likely lead to an increase of the K_I value.

In the structure of the rhGCPII/QA complex, the inhibitor mimics a glutamate-like binding mode and the nearly isosteric positioning of both molecules is aided by the atypical pyramidal geometry of the heterocyclic nitrogen atom carrying the amino acid side chain^{34–36} (Figure 3D). Since the α -amino acid fragments of the ligands structurally overlap, the increased potency of QA versus glutamate can be attributed to the distal

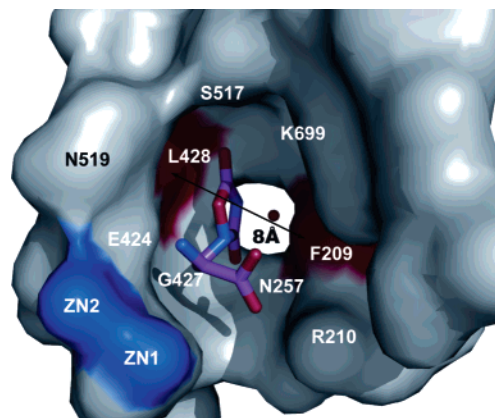


Figure 5. Schematic representation of a narrow channel contributing to the S1' pocket, with the size restricted by the side chains of Phe209 and Leu428. The S1' pocket of GCPII, defined by the residues Phe209, Arg210, Asn257, Glu424, Gly427, Leu428, Gly518, Lys699, and Tyr700, has dimensions of approximately 8 Å × 8 Å × 8 Å. The invariant positions of the Phe209 and Leu428 side chains (red) restrict the width of the pocket and, consequently, the size and placement of an S1'-bound inhibitor. The rhGCPII residues forming the S1' pocket are represented by their solvent accessible surfaces. The S1'-bound QA molecule is shown in stick representation. The residues "capping" the S1' pocket were omitted for clarity.

portions of the inhibitors. Compared to the glutamate γ -carboxylate, the oxadiazolidine ring in QA forms four additional hydrogen bonds with rhGCPII (Figure 3 and Supporting Information Table S1). Also, when compared to the side chain of glutamate, the oxadiazolidine ring is engaged in more extensive van der Waals interactions with the side chains of Phe209 and Leu428. Thus, both the polar and hydrophobic interactions contribute to the observed decrease of the quisqualate inhibition concentration value.

In contrast to the potent inhibitory properties of QA ($IC_{50} = 9.5 \mu$ M), other glutamate bioisosteres, such as AMPA and willardiine, bind GCPII with lower affinity [$IC_{50} > 10$ mM for AMPA^{37,38} and $IC_{50} = 67 \mu$ M for (*S*)-willardiine (Figure 1)]. It is noted that the acidity of the heterocyclic ring in QA is very close to that of the glutamate γ -carboxyl group ($pK_a(QA) = 4.2$; $pK_a(Glu) = 4.4$).³⁵ The heterocyclic moieties of the other bioisosteres are substantially more basic with pK_a values of 9.3 and 10.1 for willardiine and AMPA, respectively.^{39,40} Consequently, the oxadiazolidine ring in QA is negatively charged at physiological pH whereas the heterocyclic rings of the other bioisosteres are neutral. Weaker GCPII inhibition by the latter compounds indicates the importance of electrostatic interactions between an inhibitor and the enzyme.

Our data suggest that the S1' site is capable of the subtle-to-pronounced structural adjustments necessary to accommodate structurally different ligands. For example, the rearrangement of the S1' site, represented by the displacement of a loop harboring Gly518 or repositioning of the Asn257 side chain, is evident from the rhGCPII/QA structure. Similarly, slight variations could be observed in the positions of the Phe209 and Tyr700 side chains (up to ~0.5 Å) in the rhGCPII/L-SOS complex when compared to the 2-PMPA structure. At the same time, flexibility of the S1' site is limited by the overall fold of the enzyme, as all three GCPII extracellular subdomains contribute to substrate recognition. Particularly interesting is the virtually constant spacing between the side chains of the Phe209 and Leu428 located at the beginning of helices $\alpha 5$ (residues 210–219) and $\alpha 9$ (residues 429–445), respectively. These two side chains define a narrow channel with a diameter of approximately 8.0 Å (Figure 5), thus imposing limits on the

size and placement of a potential inhibitor molecule in the S1' site.

In summary, the work presented here analyzes structural features of the pharmacophore pocket of human GCPII. A limited plasticity of the S1' pocket, observed in the described structures, supports conclusions drawn from the previous SAR studies that pointed toward structural rigidity of the GCPII pharmacophore (i.e., S1') pocket¹⁸ on one hand but at the same time led to discovery of P1'-modified compounds with potent inhibitory activities toward GCPII.^{21,22} In addition, the data presented here could be exploited for the development of the novel GCPII inhibitors using the rational structure-based drug design approach. As an example, it might be feasible to substitute the γ -carboxylate group of a glutamate-containing inhibitor with a heterocyclic ring derived from a glutamate bioisoster, such as quisqualic acid or willardiine. Such modifications could improve the pharmacokinetic profile of a resulting compound (because of increased lipophilicity) as well as enhance its potency toward GCPII.

Note Added in Proof. During the editorial review of the manuscript, two of the GCPII complexes presented here were concurrently reported by Mesters and colleagues.⁴⁵

Acknowledgment. We thank Jana Starkova for excellent technical assistance. We acknowledge the use of beamlines 22BM and 22ID of the Southeast Regional Collaborative Access Team (SER-CAT), located at the Advanced Photon Source (APS), Argonne National Laboratory. Use of the APS was supported by the U.S. Department of Energy, Office of Science, Office of Basic Energy Sciences, under Contract No. W-31-109-Eng-38. The project was supported by the Intramural Research Program of the National Institutes of Health, National Cancer Institute, Center for Cancer Research (C.B. and J.L.). J.K., M.R., K.H., P.M., and A.P. were supported in part by the Ministry of Education of the Czech Republic (Research Centre for new Antivirals and Antineoplastics, Grant 1M0508).

Supporting Information Available: Figures S1–S3 and Tables T1–T3 that detail intermolecular interactions between rhGCPII and a corresponding inhibitor. This material is available free of charge via the Internet at <http://pubs.acs.org>.

References

- Doble, A. The role of excitotoxicity in neurodegenerative disease: implications for therapy. *Pharmacol. Ther.* **1999**, *81*, 163–221.
- Sacha, P.; Zámečník, J.; Barinka, C.; Hlouchova, K.; Vicha, A.; Mlcochova, P.; Hilgert, I.; Eckschlager, T.; Konvalinka, J. Expression of glutamate carboxypeptidase II in human brain. *Neuroscience* **2007**, *144*, 1361–1372.
- Troyer, J. K.; Beckett, M. L.; Wright, G. L., Jr. Detection and characterization of the prostate-specific membrane antigen (PSMA) in tissue extracts and body fluids. *Int. J. Cancer* **1995**, *62*, 552–558.
- Neale, J. H.; Olszewski, R. T.; Gehl, L. M.; Wroblewska, B.; Bzdega, T. The neurotransmitter *N*-acetylaspartylglutamate in models of pain, ALS, diabetic neuropathy, CNS injury and schizophrenia. *Trends Pharmacol. Sci.* **2005**, *26*, 477–484.
- Carpenter, K. J.; Sen, S.; Matthews, E. A.; Flatters, S. L.; Wozniak, K. M.; Slusher, B. S.; Dickenson, A. H. Effects of GCP-II inhibition on responses of dorsal horn neurones after inflammation and neuropathy: an electrophysiological study in the rat. *Neuropeptides* **2003**, *37*, 298–306.
- Ghadge, G. D.; Slusher, B. S.; Bodner, A.; Canto, M. D.; Wozniak, K.; Thomas, A. G.; Rojas, C.; Tsukamoto, T.; Majer, P.; Miller, R. J.; Monti, A. L.; Roos, R. P. Glutamate carboxypeptidase II inhibition protects motor neurons from death in familial amyotrophic lateral sclerosis models. *Proc. Natl. Acad. Sci. U.S.A.* **2003**, *100*, 9554–9559.
- Slusher, B. S.; Vornov, J. J.; Thomas, A. G.; Hurn, P. D.; Harukuni, I.; Bhardwaj, A.; Traystman, R. J.; Robinson, M. B.; Britton, P.; Lu, X. C.; Tortella, F. C.; Wozniak, K. M.; Yudkoff, M.; Potter, B. M.; Jackson, P. F. Selective inhibition of NAALADase, which converts NAAG to glutamate, reduces ischemic brain injury. *Nat. Med.* **1999**, *5*, 1396–1402.
- Olszewski, R. T.; Bukhari, N.; Zhou, J.; Kozikowski, A. P.; Wroblewski, J. T.; Shamimi-Noori, S.; Wroblewska, B.; Bzdega, T.; Vicini, S.; Barton, F. B.; Neale, J. H. NAAG peptidase inhibition reduces locomotor activity and some stereotypes in the PCP model of schizophrenia via group II mGluR. *J. Neurochem.* **2004**, *89*, 876–885.
- Wroblewska, B.; Wroblewski, J. T.; Pshenichkin, S.; Surin, A.; Sullivan, S. E.; Neale, J. H. *N*-Acetylaspartylglutamate selectively activates mGluR3 receptors in transfected cells. *J. Neurochem.* **1997**, *69*, 174–181.
- Thomas, A. G.; Liu, W.; Olkowski, J. L.; Tang, Z.; Lin, Q.; Lu, X. C.; Slusher, B. S. Neuroprotection mediated by glutamate carboxypeptidase II (NAALADase) inhibition requires TGF- β . *Eur. J. Pharmacol.* **2001**, *430*, 33–40.
- Bruno, V.; Wroblewska, B.; Wroblewski, J. T.; Fiore, L.; Nicoletti, F. Neuroprotective activity of *N*-acetylaspartylglutamate in cultured cortical cells. *Neuroscience* **1998**, *85*, 751–757.
- Barinka, C.; Rinnova, M.; Sacha, P.; Rojas, C.; Majer, P.; Slusher, B. S.; Konvalinka, J. Substrate specificity, inhibition and enzymological analysis of recombinant human glutamate carboxypeptidase II. *J. Neurochem.* **2002**, *80*, 477–487.
- Serval, V.; Galli, T.; Cheramy, A.; Glowinski, J.; Lavielle, S. In vitro and in vivo inhibition of *N*-acetyl-L-aspartyl-L-glutamate catabolism by *N*-acylated L-glutamate analogs. *J. Pharmacol. Exp. Ther.* **1992**, *260*, 1093–1100.
- Subasinghe, N.; Schulte, M.; Chan, M. Y.; Roon, R. J.; Koerner, J. F.; Johnson, R. L. Synthesis of acyclic and dehydroaspartic acid analogues of Ac-Asp-Glu-OH and their inhibition of rat brain *N*-acetylated alpha-linked acidic dipeptidase (NAALA dipeptidase). *J. Med. Chem.* **1990**, *33*, 2734–2744.
- Jackson, P. F.; Cole, D. C.; Slusher, B. S.; Stetz, S. L.; Ross, L. E.; Donzanti, B. A.; Trainor, D. A. Design, synthesis, and biological activity of a potent inhibitor of the neuropeptidase *N*-acetylated alpha-linked acidic dipeptidase. *J. Med. Chem.* **1996**, *39*, 619–622.
- Kozikowski, A. P.; Nan, F.; Conti, P.; Zhang, J.; Ramadan, E.; Bzdega, T.; Wroblewska, B.; Neale, J. H.; Pshenichkin, S.; Wroblewski, J. T. Design of remarkably simple, yet potent urea-based inhibitors of glutamate carboxypeptidase II (NAALADase). *J. Med. Chem.* **2001**, *44*, 298–301.
- Wone, D. W.; Rowley, J. A.; Garofalo, A. W.; Berkman, C. E. Optimizing phenylethylphosphonamidates for the inhibition of prostate-specific membrane antigen. *Bioorg. Med. Chem.* **2006**, *14*, 67–76.
- Jackson, P. F.; Tays, K. L.; Maclin, K. M.; Ko, Y. S.; Li, W.; Vitharana, D.; Tsukamoto, T.; Stoermer, D.; Lu, X. C.; Wozniak, K.; Slusher, B. S. Design and pharmacological activity of phosphinic acid based NAALADase inhibitors. *J. Med. Chem.* **2001**, *44*, 4170–4175.
- Majer, P.; Jackson, P. F.; Delahanty, G.; Grella, B. S.; Ko, Y. S.; Li, W.; Liu, Q.; Maclin, K. M.; Polakova, J.; Shaffer, K. A.; Stoermer, D.; Vitharana, D.; Wang, E. Y.; Zakrzewski, A.; Rojas, C.; Slusher, B. S.; Wozniak, K. M.; Burak, E.; Limsakun, T.; Tsukamoto, T. Synthesis and biological evaluation of thiol-based inhibitors of glutamate carboxypeptidase II: discovery of an orally active GCP II inhibitor. *J. Med. Chem.* **2003**, *46*, 1989–1996.
- Stoermer, D.; Liu, Q.; Hall, M. R.; Flanary, J. M.; Thomas, A. G.; Rojas, C.; Slusher, B. S.; Tsukamoto, T. Synthesis and biological evaluation of hydroxamate-based inhibitors of glutamate carboxypeptidase II. *Bioorg. Med. Chem. Lett.* **2003**, *13*, 2097–2100.
- Ding, P.; Miller, M. J.; Chen, Y.; Helquist, P.; Oliver, A. J.; Wiest, O. Syntheses of conformationally constricted molecules as potential NAALADase/PSMA inhibitors. *Org. Lett.* **2004**, *6*, 1805–1808.
- Majer, P.; Hin, B.; Stoermer, D.; Adams, J.; Xu, W.; Duvall, B. R.; Delahanty, G.; Liu, Q.; Stathis, M. J.; Wozniak, K. M.; Slusher, B. S.; Tsukamoto, T. Structural optimization of thiol-based inhibitors of glutamate carboxypeptidase II by modification of the P1' side chain. *J. Med. Chem.* **2006**, *49*, 2876–2885.
- Davis, M. I.; Bennett, M. J.; Thomas, L. M.; Bjorkman, P. J. Crystal structure of prostate-specific membrane antigen, a tumor marker and peptidase. *Proc. Natl. Acad. Sci. U.S.A.* **2005**, *102*, 5981–5986.
- Mesters, J. R.; Barinka, C.; Li, W.; Tsukamoto, T.; Majer, P.; Slusher, B. S.; Konvalinka, J.; Hilgenfeld, R. Structure of glutamate carboxypeptidase II, a drug target in neuronal damage and prostate cancer. *EMBO J.* **2006**, *25*, 1375–1384.

- (25) Otwinowski, Z.; Minor, W. Processing of X-ray Diffraction Data Collected in Oscillation Mode. In *Methods in Enzymology*; Carter Jr., C. W., Sweet, R. M., Eds.; Academic Press: New York 1997; Vol. 276, pp 307–326.
- (26) Barinka, C.; Starkova, J.; Konvalinka, J.; Lubkowski, J. A high-resolution structure of ligand-free glutamate carboxypeptidase II. *Acta Crystallogr. F* **2007**, *63*, 150–153.
- (27) Murshudov, G. N.; Vagin, A. A.; Lebedev, A.; Wilson, K. S.; Dodson, E. J. Efficient anisotropic refinement of macromolecular structures using FFT. *Acta Crystallogr. D* **1999**, *55*, 247–255.
- (28) McRee, D. E. XtalView/Xfit. A versatile program for manipulating atomic coordinates and electron density. *J. Struct. Biol.* **1999**, *125*, 156–165.
- (29) Laskowski, R. A.; McArthur, M. W.; Moss, D. S.; Thornton, J. M. PROCHECK: a program to check the stereochemical quality of protein structures. *J. Appl. Crystallogr.* **1993**, *26*, 283–291.
- (30) Collaborative Computational Project, Number 4. “The CCP4 Suite: Programs for Protein Crystallography”. *Acta Crystallogr. D* **1994**, *50*, 760–763.
- (31) Serval, V.; Barbeito, L.; Pittaluga, A.; Cheramy, A.; Lavielle, S.; Glowinski, J. Competitive inhibition of N-acetylated-alpha-linked acidic dipeptidase activity by N-acetyl-L-aspartyl-beta-linked L-glutamate. *J. Neurochem.* **1990**, *55*, 39–46.
- (32) Robinson, M. B.; Blakely, R. D.; Coyle, J. T. Quisqualate selectively inhibits a brain peptidase which cleaves N-acetyl-L-aspartyl-L-glutamate in vitro. *Eur. J. Pharmacol.* **1986**, *130*, 345–347.
- (33) Vitharana, D.; France, J. E.; Scarpetti, D.; Bonneville, G. W.; Majer, P.; Tsukamoto, T. Synthesis and biological evaluation of (R)- and (S)-2-(phosphonomethyl)pentanedioic acids as inhibitors of glutamate carboxypeptidase II. *Tetrahedron: Asymmetry* **2002**, *13*, 1609–1614.
- (34) Flippen, J. L.; Gilardi, R. D. Quisqualic acid. *Acta Crystallogr. B* **1976**, *32*, 951–953.
- (35) Boden, P.; Bycroft, B. W.; Chhabra, S. R.; Chiaplín, J.; Crowley, P. J.; Grout, R. J.; King, T. J.; McDonald, E.; Rafferty, P.; Usherwood, P. N. The action of natural and synthetic isomers of quisqualic acid at a well-defined glutamatergic synapse. *Brain Res.* **1986**, *385*, 205–211.
- (36) Jackson, D. E.; Bycroft, B. W.; King, T. J. Crystallographic studies and semi-empirical MNDO calculations on quisqualic acid and its analogs. Systems containing unusual pyramidal heterocyclic ring nitrogens. *J. Comput.-Aided Mol. Des.* **1989**, *2*, 321–328.
- (37) Tiffany, C. W.; Cai, N. S.; Rojas, C.; Slusher, B. S. Binding of the glutamate carboxypeptidase II (NAALADase) inhibitor 2-PMPA to rat brain membranes. *Eur. J. Pharmacol.* **2001**, *427*, 91–96.
- (38) Robinson, M. B.; Blakely, R. D.; Couto, R.; Coyle, J. T. Hydrolysis of the brain dipeptide N-acetyl-L-aspartyl-L-glutamate. Identification and characterization of a novel N-acetylated alpha-linked acidic dipeptidase activity from rat brain. *J. Biol. Chem.* **1987**, *262*, 14498–14506.
- (39) Matzen, L.; Engesgaard, A.; Ebert, B.; Didriksen, M.; Frolund, B.; Krosgaard-Larsen, P.; Jaroszewski, J. W. AMPA receptor agonists: synthesis, protolytic properties, and pharmacology of 3-isothiazolol bioisosteres of glutamic acid. *J. Med. Chem.* **1997**, *40*, 520–527.
- (40) Hill, R. A.; Wallace, L. J.; Miller, D. D.; Weinstein, D. M.; Shams, G.; Tai, H.; Layer, R. T.; Willins, D.; Uretsky, N. J.; Danthi, S. N. Structure–activity studies for alpha-amino-3-hydroxy-5-methyl-4-isoxazolepropanoic acid receptors: acidic hydroxyphenylalanines. *J. Med. Chem.* **1997**, *40*, 3182–3191.
- (41) Kraulis, P. E. MOLSCRIPT: a program to produce both detailed and schematic plots of protein structures. *J. App. Crystallogr.* **1991**, *24*, 946–950.
- (42) Esnouf, R. M. Further additions to MolScript version 1.4, including reading and contouring of electron-density maps. *Acta Crystallogr. D* **1999**, *55*, 938–940.
- (43) Merritt, E. A.; Murphy, M. E. Raster3D version 2.0. A program for photorealistic molecular graphics. *Acta Crystallogr. D* **1994**, *50*, 869–873.
- (44) DeLano, W. L. *The PyMOL Molecular Graphics System*; Delano Scientific: Palo Alto, CA, 2002.
- (45) Mesters, J.R.; Henning, K.; Hilgenfeld, R. Human glutamate carboxypeptidase II inhibition: structures of GCPII in complex with two potent inhibitors, quisqualate and 2-PMPA. *Acta Crystallogr. D* **2007**, *63*, 508–513.

JM070133W